Pak. J. Engg. & Appl. Sci. Vol. 18 January, 2016 (*p.* 98–110)

Empirical Estimation of Unconfined Compressive Strength and Modulus of Elasticity Using ANN

Hasan Gul[1], Khalid Farooq[2] and Hassan Mujtaba[3]

1. *Department of Civil Engineering, University of Engineering and Technology, Lahore, Pakistan*
2. *Department of Civil Engineering, University of Engineering and Technology, Lahore, Pakistan*
3. *Department of Civil Engineering, University of Engineering and Technology, Lahore, Pakistan*

* **Corresponding Author:** E-mail: *hassaninbox@gmail.com*

Abstract

The strength parameters such as unconfined compressive strength (UCS) and Modulus of Elasticity (E) of rocks are important for design of foundations. Both the parameters are determined in laboratory after rigorous and destructive testing. In this study Artificial Neural Network (ANN) models are developed for prediction of UCS and E from index test parameters such as Unit Weight (γ), porosity (n) and point load index $I_{s(50)}$. Multi variable regression models are also developed to compare the accuracy of prediction from different models. Coefficient of determination (R^2), Root Mean Squared error (RMSE) and Standard Error of Estimate (SEE) has been used as the controlling factor to determine the prediction accuracy of both ANN and multivariable regression. The ANN models increased the R^2 values from 0.53 to 0.72 and 0.51 to 0.75 for UCS and E respectively. The variation between experimental and predicted values of UCS and E for ANN model are ± 23% and ± 29% and for regression model are ± 40% and ± 31% respectively.

Key Words: Artificial neural network, multivariable regression, unconfined compressive strength, Modulus of Elasticity

1. Introduction

Foundation of various civil engineering structures such as roads, bridges, tunnels, dams, harbors and high rise buildings are constructed up to natural rock beds. Therefore, it becomes important to analyze the behavior of rocks under the loads transferred from various structures on them. Unconfined compressive strength (UCS) and Modulus of Elasticity (E) are obligatory parameters for geotechnical design and evaluation of rock behavior. These measurement necessitates the recovery of high quality core specimen from the field. In laboratory rigorous and destructive tests are performed on the test specimens. At prefeasibility and preliminary design stages, these procedures are costly and time consuming. Therefore, it is preferred that indirect test methods may be used for the prediction of UCS and E. Artificial Neural Network (ANN) is being used as an alternate of statistical analysis for prediction of unknown geotechnical parameters. Its prediction accuracy is higher and it models real time complex field problems. ANN is mathematical models consisting of neurons in different layers. ANN is similar to biological neurons in human brain, which are interconnected with other neurons in subsequent layers [1]. The neurons communicate with each other by sending a signal over a large array of interconnected neurons having biased and weighted connections. A typical neural network model consists of input layer, hidden layer and output layer. Each of the layers consists of different number of neurons and has its own weights and biases. The weights and biases are adjusted during the training of ANN [2]. Various researchers [3], [4], [5], [6], [9], [13] and [15] have proposed empirical models to predict UCS and E from index test parameters.

Neural Network model is developed using feed forward back propagation algorithm with four layers, input layer of 4 neurons, two hidden layers of 20, 30 neurons and one output layer of 2 neurons [3]. The outputs from multivariable regression equation are compared with outputs of neural network. It is noted that neural network predicted regression coefficients of 0.96 for E and 0.93 for UCS of gypsum rock from input parameters of slake durability index, point load index, effective porosity and Schmidt hammer hardness. The performance indices such as root mean square error (RMSE) and variance account for (VAF) are 2.65, 2.28 and 92, 91 for UCS and E, respectively. In other study carbonate rock samples are collected from various stone processing plants in Turkey [4]. The laboratory tests were carried for the development of prediction models for UCS from Schmidt hammer test. In the comparative analysis of

results obtained from regression analysis and neural network model coefficient of determination (R^2), RMSE, VAF indices are 0.39, 46.51, 12.45 for regression and 0.96, 7.92, 95.84 for neural network model. It shows the prediction accuracy of ANN is significantly better than the regression analysis. Carbonate rock travertine and limestone from the villages in Kaklik, Kocabas, Honaz in Danzili Basin, Turkey for the study are collected [5]. A neural feed forward propagation model is developed having network architecture of input layer 5 neurons, hidden layer 2 neurons and output layer 2 neurons. UCS and E parameters are predicted from five rock properties namely dry unit weight, effective porosity, Schmidt hardness rebound number, p-wave velocity and slake durability cycles. Multi regression models are also developed for comparison. Results showed that R^2 is 0.55 for regression model and 0.66 for ANN model predicting UCS. R^2 is 0.66 for regression and 0.72 for ANN model predicting E. The neural network model gave precise values as average performance indices are higher than regression model. Neural Network model with feed forward back propagation training algorithm for prediction of UCS of rocks is developed [6]. Rock samples are collected from various coal fields in Iran and the standard cores are extracted to perform laboratory tests. The 93 number dataset including Schmidt hardness, density, porosity and UCS parameters is developed from laboratory test. The ANN model R^2, VAF and mean absolute error (Ea) and mean relative error (Er) are calculated as 97.25%, 95.65,%, 0.0942 MPa, 1.1127% respectively, 89.88%, 91.61%, 0.1117 MPa, 2.3422 are calculated for regression model. The ANN models performance indices indicate better results than the models developed from the regression. In this study effort has been made to develop predictive models for the estimation of UCS and E from rock type (RN), unit weight (γ), porosity (n) and point load index $I_{s(50)}$

2. Sampling Location

The Kohala hydro power project is located in Muzaffarabad district, and the dam site is on Jhelum River. The area has large formations of sedimentary rocks. It mainly includes Sand stone and Shale rock. The Basha dam site is located in northern area in Kohistan, Pakistan. The sampling location is shown in Figure 1. At dam site the rock formation are of mafic intrusive rocks which include mainly two types of rock i.e. Gabbronorite and Ultramafic Association. In order to determine strength characteristics of rock formations a detailed in-situ and laboratory testing plan is proposed. The UCS, E and other index test parameters are determined in laboratory by the test procedures outlined by American Society of Testing and Materials [8]. Numerical description of rock type is given in Table 1 and the database of 143 dataset is presented in Table 2. Pictorial view of rock samples and testing is shown in Figure 2.

Table 1 Numerical description of rock samples; (Gul, 2015)

Rock Number	Rock Type (RN)	Unit Weight (kN/m^3)
1	Ultramaffic Association	27.37 – 34.14
2	Gabbronorite	26.87 – 33.45
3	Sand Stone	22.46 – 28.45
4	Shale	24 – 24.07

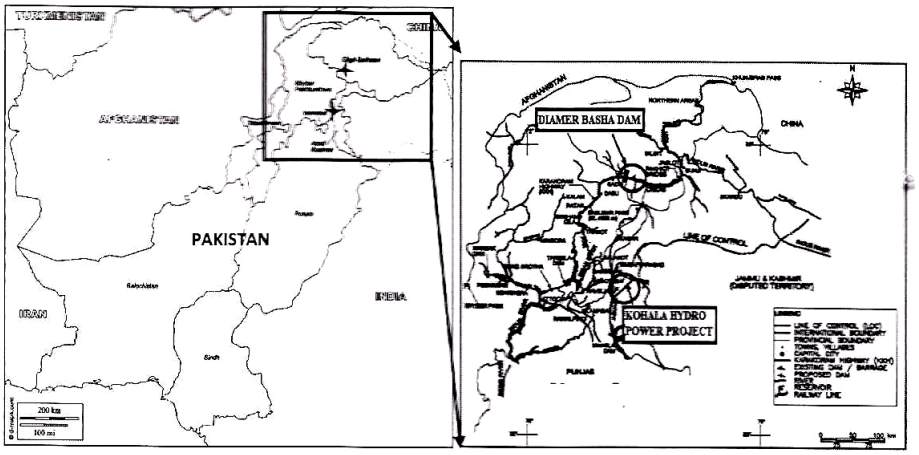

Fig. 1 Sampling Location at Diamer Basha dam and Kohala hydro power station sites; (Munir, 2014)

Table 2 Dataset prepared from laboratory tests; (Gul, 2015)

Sr. No.	Sample number	Rock type	Depth (m)	ã (kN/m^3)	n (%)	$Is_{(50)}$ (MPa)	UCS (MPa)	E (GPa)
1	G-35	UMA	27.68-28.12	32.08	3.430	2.55	60	29.39
2	G-36	UMA	30.72-30.90	30.21	2.760	2.19	30	17.91
3	G-40	UMA	39.40-39.57	29.04	2.110	9.21	87	78.41
4	G-41	UMA	45.57- 46.04	32.96	1.500	1.98	62	26.53
5	G-42	UMA	55.00-55.63	32.96	1.150	3.16	61	33.42
6	G-43	UMA	58.17-58.50	31.10	1.100	4.39	58	40.01
7	G-44	UMA	65.43-65.90	32.77	1.430	3.07	46	28.23
8	G-45	UMA	65.00-65.25	32.08	2.000	2.63	45	25.23
9	G-46	UMA	66.92-67.10	34.14	2.170	2.33	15	14.13
10	G-47	Gabbronorite	73.08-73.48	27.76	0.650	6.95	102	69.25
11	G-48	UMA	75.00-75.14	32.08	5.940	2.3	34	19.82
12	G-49	UMA	79.53-79.89	33.65	2.020	3.92	75	42.40
13	G-50	Gabbronorite	96.32-96.84	31.98	3.350	7.67	102	73.65
14	G-51	Gabbronorite	103.64-104.33	32.18	2.920	11.85	62	86.81
15	G-52	UMA	106.17-106.55	32.37	0.510	7.54	70	62.96
16	G-53	Gabbronorite	110.07 -110.35	33.16	2.600	2.67	50	27.03
17	G-54	Gabbronorite	117.00-117.46	33.45	1.180	5.84	96	60.62
18	G-55	UMA	34.23-34.53	30.51	2.350	11.26	112	73.62
19	G-56	UMA	34.65-34.80	31.20	0.790	1.71	75	28.90
20	G-57	UMA	29.23-29.60	34.04	1.460	2.61	53	27.59
21	G-58	Gabbronorite	117.99-118.33	32.47	2.330	5.47	53	45.06
22	G-59	UMA	107.25-107.55	32.77	1.620	2.32	96	39.63
23	G-61	Gabbronorite	30.00 - 30.30	29.53	0.812	9.21	106	67.6
24	G-62	Gabbronorite	49.27 - 49.53	29.18	2.390	9.05	95	58
25	G-63	Gabbronorite	51.75 - 52.00	28.56	1.570	6.48	128	38.3
26	G-64	Gabbronorite	127.53 - 127.65	28.01	1.310	7.85	94	58
27	G-65	Gabbronorite	49.65 - 50.00	27.55	0.850	11.54	120	72
28	G-66	Gabbronorite	35.08 - 35.35	27.76	2.640	9	94	93.2
29	G-67	Gabbronorite	51.78 - 52.09	27.95	2.140	11.2	103	98.1
30	G-68	Gabbronorite	30.50 - 30.74	28.34	2.870	11.69	108	101
31	G-69	Gabbronorite	95.50 - 95.76	28.27	1.970	7.03	117	59.5
32	G-70	Gabbronorite	95.76 - 96.00	28.54	1.640	5.23	116	41.3
33	G-71	Gabbronorite	101.62 - 101.90	27.82	1.240	7.01	90	69.2
34	G-72	Gabbronorite	116.54-116.85	28.06	0.550	9.12	113	91
35	G-73	Gabbronorite	130.40 - 130.65	28.17	0.870	5.68	129	50.6
36	G-74	Gabbronorite	130.65 - 130.9	28.31	0.560	7	143	69
37	G-75	Gabbronorite	58.33 - 58.58	26.87	1.271	5.91	117	49.7
38	G-76	Gabbronorite	37.25 - 37.48	27.66	1.238	6.45	92	28.6
39	G-77	Gabbronorite	37.48 - 37.75	27.76	1.206	7.8	109	73
40	G78	Gabbronorite	99.67 - 99.95	27.62	1.173	6.82	90	79.1
41	G-79	Gabbronorite	143.50 - 143.82	27.24	1.140	6.17	116	72.8
42	G-80	Gabbronorite	30.35 - 30.61	27.57	1.107	5.8	72	30.1
43	G-81	Gabbronorite	27.36 - 37.61	27.47	1.074	3.34	75	32.9
44	G-82	Gabbronorite	130.02 - 130.62	27.68	1.041	3.71	63	37.8
45	G83	Gabbronorite	50.93 - 51.20	27.76	1.008	7.54	95	53.7
46	G-84	Gabbronorite	75.25 - 75.52	27.37	0.976	4.6	91	42
47	G85	Gabbronorite	156.28 - 156.55	26.98	0.943	4.14	87	18.5
48	G-86	Gabbronorite	156.55 - 156.83	27.80	0.910	3.36	71	20.4
49	G-87	Gabbronorite	82.60 - 82.90	27.45	0.877	1.71	46	11.2
50	G-88	Gabbronorite	35.60 - 35.85	27.11	0.844	3.1	69	3.7
51	G-89	Gabbronorite	35.85 - 36.11	26.93	0.811	3.41	75	23.7
52	G-90	Gabbronorite	59.30-59.78	28.25	0.426	7.26	123	77.58
53	G-91	Gabbronorite	92.52-92.98	28.65	0.319	5.4	80	52.94
54	G-92	Gabbronorite	68.50-68.85	28.25	1.230	6.76	80	68.3
55	G-93	Gabbronorite	84.12-84.54	28.65	0.649	10.26	96	65
56	G-94	Gabbronorite	100.01-100.37	28.84	0.369	14	148	98
57	G-95	Gabbronorite	104.1-104.47	28.65	0.783	9.71	127	37.1
58	G-96	Gabbronorite	152.78-153.13	28.74	0.679	10.29	133	88
59	G-97	Gabbronorite	155.1-155.55	28.84	0.568	10.87	126	77

Table 2 Continued

Table 2 Continued

Sr.	Sample number	Rock type	Depth (m)	ã (kN/m^3)	n (%)	$Is_{(50)}$ (MPa)	UCS (MPa)	E (GPa)
60	G-98	Gabbronorite	166.44-166.81	28.84	0.565	7.84	88	45.7
61	G-99	Gabbronorite	168.60-169.01	29.23	0.771	10.57	100	86.4
62	G-100	UMA	27.29-27.63	28.06	1.402	11.06	125	95.6
63	G-101	UMA	27.24-27.54	27.96	0.306	10.2	115	77
64	G-102	UMA	33.92-34.14	27.37	1.270	8.08	115	85.8
65	G-103	UMA	36.97-37,27	27.57	1.536	9.36	138	114
66	G-104	UMA	39.47-39.74	27.76	0.442	10.87	104	55
67	G-105	UMA	52.55-52.86	28.06	0.513	10.78	124	82
68	G-106	UMA	54.50-54.78	29.14	0.196	11.64	126	84
69	G-107	UMA	55.05-55.35	28.06	0.615	11.54	126	84
70	G-108	UMA	56.72-57.01	28.74	0.503	12.6	124	101
71	G-109	UMA	62.71-62.95	28.35	1.655	9.03	78	13.2
72	G-110	UMA	117.66-118.00	32.67	0.351	9.66	113	73
73	G-111	UMA	121.45-121.72	32.27	1.006	8.12	89	88.3
74	G-112	UMA	107.47-107.78	32.18	1.615	6.35	80	76.3
75	G-113	UMA	48.00-48.32	28.35	0.963	8.39	74	36.9
76	G-114	UMA	44.64-45.00	32.08	0.589	10.31	111	57.8
77	G-115	Gabbronorite	124.6-124.93	29.14	0.512	12.18	130	47
78	G-116	Gabbronorite	162.14-162.42	28.65	0.441	9.52	110	66
79	G-117	Gabbronorite	187.97-188.34	28.35	1.148	6.14	74	16.5
80	G-118	Gabbronorite	77.64-78.00	28.65	0.743	6.35	58	13.5
81	G-119	Gabbronorite	131.64-132.00	28.25	1.134	3.39	99	23
82	G-120	Gabbronorite	138.00-138.35	28.45	0.926	5.93	81	40.3
83	G-121	Gabbronorite	72.29-72.59	28.35	1.081	6.79	85	43.2
84	G-122	Gabbronorite	43.58-43.95	28.55	0.317	10.78	108	73.6
85	G-123	Gabbronorite	75.00-75.32	28.45	0.788	7.93	71	26.3
86	G-124	Gabbronorite	107.85-108.15	28.65	0.821	7.26	86	59
87	G-125	Gabbronorite	122.09-122.46	29.14	1.271	7.93	89	27.9
88	G-126	Gabbronorite	144.38-144.72	28.65	1.025	5.62	47	42.4
89	G-127	Gabbronorite	49.02-49.32	28.94	0.678	7.48	68	55.4
90	G-128	Gabbronorite	96.03-96.32	28.94	0.669	11.79	158	114
91	G-129	Gabbronorite	90.07-90.38	28.94	0.137	10.97	121	73
92	G-130	Gabbronorite	90.64-90.93	29.04	0.312	11.24	161	106
93	G-131	Gabbronorite	136.74-137.03	29.23	0.494	10.31	114	24.3
94	G-132	Gabbronorite	145.10-145.43	29.23	0.535	7.48	121	51.3
95	G-133	Gabbronorite	46.13-46.42	29.14	0.642	11.29	121	45
96	G-134	Gabbronorite	70.95-71.29	28.45	0.626	10.47	74	27.5
97	G-135	Gabbronorite	165.16-165.47	28.06	0.804	9.02	83	35.8
98	G-136	Gabbronorite	79.71-79.99	28.06	0.335	9.97	148	56.9
99	G-137	Gabbronorite	37.67-38.02	28.65	0.403	10.95	92	56.9
100	G-138	Gabbronorite	34.51-34.82	28.55	0.388	10.63	91	55.1
101	G-139	Gabbronorite	49.28-49.59	28.74	0.335	12.44	128	85
102	BH2-1	Sand Stone	61.60	24.15	3.300	5.00	21.56	32.46
103	BH2-3	Sand Stone	65.00	24.65	2.400	6.11	75.00	38.29
104	BH2-8	Sand Stone	89.20	26.00	3.300	9.44	75.00	37.79
105	BH2-10	Sand Stone	102.50	25.00	4.000	6.39	27.45	42.77
106	BH15-3B	Sand Stone	50.30	25.89	7.400	0.83	48.60	15.36
107	BH15-3C	Sand Stone	50.50	26.00	3.500	2.78	61.00	47.07
108	BH15-4	Sand Stone	55.70	26.34	6.100	3.61	74.20	40.25
109	BH15-11	Sand Stone	89.20	26.76	4.200	6.11	52.00	31.63
110	BH15-13	Sand Stone	105.10	27.00	5.400	5.00	31.60	35.56
111	BH10-5	Sand Stone	31.00	27.12	6.000	4.86	45.57	39.03
112	BCD1-1	Sand Stone	188.50	27.56	4.000	8.33	115.63	81.89
113	BCD1-5	Sand Stone	264.30	28.12	4.800	3.61	38.55	29.22
114	BCD1-5	Sand Stone	265.10	28.12	5.000	1.00	23.00	11.60

Table 2 Continued

Table 2 Continued

Sr.	Sample number	Rock type	Depth (m)	ã (kN/m^3)	n (%)	$Is_{(50)}$ (MPa)	UCS (MPa)	E (GPa)
115	BCD2-1	Sand Stone	96.30	28.00	4.560	3.33	42.84	28.84
116	BH4-9	Sand Stone	52.60	27.89	3.000	7.54	79.00	26.46
117	BH5-5	Sand Stone	89.80	28.45	5.800	3.07	65.81	34.36
118	BH21-1	Sand Stone	34.00	28.00	3.200	1.25	14.82	7.47
119	BH23-2	Sand Stone	56.20	27.76	4.000	5.24	68.60	48.54
120	BH28-1	Sand Stone	41.50	26.87	7.100	5.23	24.82	34.87
121	BH31-1	Sand Stone	29.20	27.50	3.100	4.25	13.36	25.34
122	BH09-1	Sand Stone	18.50	25.00	3.800	3.61	33.15	27.56
123	BH09-7	Shale	28.10	24.07	6.100	5.55	73.00	31.49
124	BH09-9	Sand Stone	37.80	27.14	2.500	3.05	92.59	42.47
125	BH09-15	Sand Stone	70.20	27.34	3.600	6.39	61.00	25.54
126	BH18A-1	Sand Stone	22.30	28.14	3.150	2.78	68.58	33.45
127	BH18A-2	Sand Stone	35.80	25.00	5.500	4.44	33.72	32.80
128	BH18A-5	Sand Stone	72.10	24.17	6.000	4.16	30.00	7.11
129	BH18A-9	Sand Stone	78.20	24.11	7.200	2.50	58.00	13.24
130	BH18A-15	Sand Stone	87.40	28.34	2.890	4.44	81.00	15.10
131	BH26-1	Sand Stone	95.70	27.21	3.780	6.66	37.15	47.42
132	BH26-2	Sand Stone	130.40	24.00	5.900	2.22	27.43	17.29
133	BH26-6c	Sand Stone	253.80	26.76	3.230	7.22	59.44	57.74
134	BH26-14b	Shale	338.80	24.00	6.230	10.00	71.00	61.46
135	BH11-1	Sand Stone	22.20	26.50	4.210	3.37	40.00	20.23
136	BH11-3	Sand Stone	29.50	23.74	5.400	6.18	34.28	43.60
137	BH11-8	Sand Stone	48.40	26.14	4.560	11.80	113.51	102.43
138	BH01-2	Sand Stone	33.50	23.50	2.890	1.62	11.21	8.62
139	BH01-3	Sand Stone	39.20	26.00	5.000	2.34	36.00	31.19
140	BH01-22	Sand Stone	106.30	23.24	3.400	3.03	18.00	21.61
141	BH03-9	Sand Stone	60.60	23.12	6.400	4.13	18.00	11.97
142	BH14-8	Sand Stone	167.30	22.46	5.470	2.48	27.00	51.68
143	BH16-6	Sand Stone	51.30	23.00	7.000	3.58	22.00	17.16

(a)

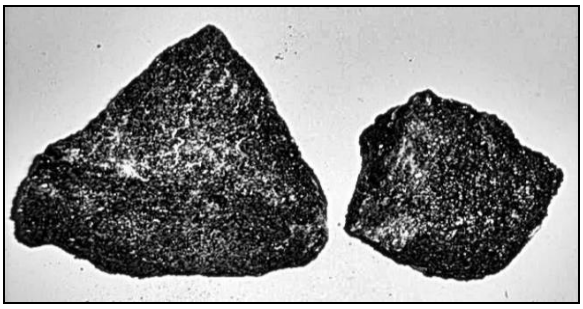

(b)

(c)

Fig. 2 Rock samples (a) Gabbronotite rock (b) UMA rock (c) Rock cores of Sand Stone and Shale (d) UCS test in progress on rock sample (Munir, 2014)

3. Statistical Analysis of Dataset

The maximum, minimum, average and standard deviation of the dataset are shown in Table 3. The standard deviation between values of $I_{s(50)}$, UCS and E is 3.23 MPa, 35.24 MPa and 27.1 GPa, respectively. It shows that mechanical behavior of rock is variable due to geological conditions of individual project sites. However prediction accuracy of mathematical models increase when data is normally distributed and outlier values are less significant [10]. The histogram plots are shown in Figure 3.

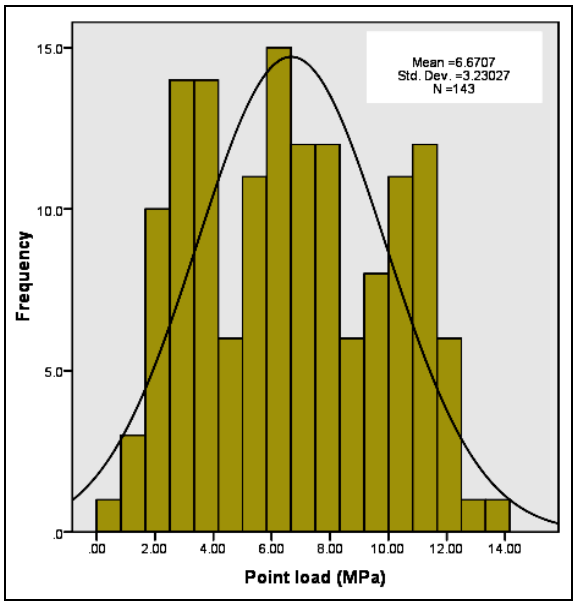

(a)

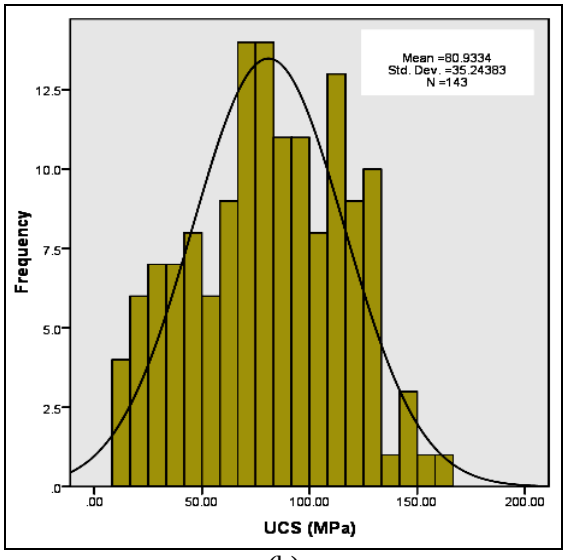

(b)

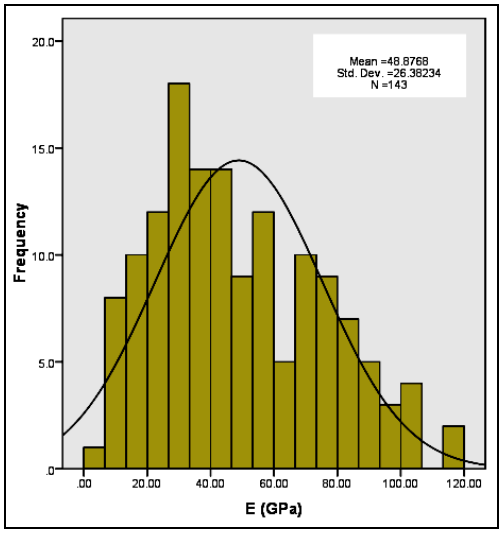

(c)

Fig. 3 Histogram plots of (a) $I_{s(50)}$ (b) UCS (c) E

Table 3 Summary of statistical values of Inputs and Outputs parameters

Statistical Analysis of Dataset (*N*=143)					
Para-meters	Ã (kN/m^3)	n (%)	$I_{s(50)}$ (MPa)	UCS (MPa)	E (GPa)
Max.	34.14	7.40	14	161	114
Min.	22.46	0.14	0.83	11.21	3.7
Avg.	28.29	2.19	6.67	80.93	49.3
St.dev.	2.39	1.90	3.23	35.24	27.1
Range	22.46 – 34.14	0.14 – 7.40	0.83 - 14	11.21 – 161	3.7 - 114

3.1 Selection of Inputs Parameters for Model

The coefficient of correlation (*R*) between different parameters rock number, unit weight, porosity, point load, unconfined compressive strength and modulus of elasticity is shown in Table 4. The absolute value of *R* near to 1 shows good correlation and near to zero show weak correlation between individual parameters. These observations are presented in past studies for prediction of compaction parameters of coarse grained soils [11]. The parameter UCS cross correlation with RN, ã, n, $I_{s(50)}$ gave values of *R*-0.40, 0.23, -0.64 and 0.73 respectively. The parameter E cross correlation with RN, ã, n, $I_{s(50)}$, UCS gave values of *R* -0.30, 0.15, -0.38, 0.71 and 0.71, respectively. The weak value of correlation is observed for parameter ã with UCS and E.

Table 4: Cross correlation between parameters of dataset (*N*=143)

	RN	ã (kN/m^3)	n (%)	$I_{s(50)}$ (MPa)	UCS (MPa)	E (GPa)
RN	1					
ã (kN/m^3)	-0.72	1				
n (%)	0.67	-0.48	1			
$I_{s(50)}$ (MPa)	-0.26	0.09	-0.48	1		
UCS (MPa)	-0.40	0.23	-0.64	0.73	1	
E (GPa)	-0.30	0.15	-0.38	0.71	0.71	1

4. Data Analysis

In this study the data is analyzed by using two techniques, Multivariable regression analysis (MVRA) and ANN to compare the prediction accuracy of models. In MVRA, mathematical equations are developed to predict the dependent variable (UCS and E) from the independent variables (rock number, unit weight, porosity and point load strength). The statistical software package SPSS 16 is used to develop regression models. The regressions equations are shown in Table 5. The increase in number of input variables has relatively produced higher regression coefficients. Model 3 and Model 6 equation has R^2 value of 0.64 and 0.65 respectively. This indicated that 65% of the data used for model development can be estimated using these MVRA models.

Table 5 MVRA equations for the prediction of UCS and E

Para-meter	Model	Equation	R^2
UCS	Model 1	$UCS = 8(I_{3(50)}) + 27.61$	0.53
	Model 2	$UCS = -10.78(RN) + 7.36 (I_{3(50)}) + 54.4$	0.58
	Model 3	$UCS = -0.51(RN) - 0.0099(\gamma) -6.9(n) + 6.03(I_{3(50)}) + 57.17$	0.64
E	Model 1	$E = 0.54(UCS) + 5.46$	0.51
	Model 2	$E = 4.03(I_{3(50)}) + 0.27(UCS) - 0.49$	0.62
	Model 3	$E = -4.32(RN) - 0.66(\gamma) + 3.52(n) + 4.16(I_{3(50)}) - 0.33 (UCS) + 23$	0.65

4.1 ANN Model Development

A multi layer neural network (MLNN) consists of three layers namely; input layer, hidden layer and output layer as mentioned earlier. The training algorithm feed forward back propagation is used for training the dataset. Weight and biases are adjustable parameters of ANN structure which are fine tuned by training algorithm keeping in view the input and the target output values to make the neural network fit the dataset. The data from the input layer is sent to hidden layer. It is summed up after applying weight and biases [12]. The general ANN equation is shown in Equation 1.

$$P = f_n\left[b_o + \sum_{k=1}^{n}\left\{ w_k f_n\left(b_{hk} + \sum_{i=1}^{m} w_{ik} X_i \right)\right\}\right] \quad (1)$$

Where f_n is the transfer function, h is the number of neurons in hidden layer, x_i is the input value, m is number of input variables, w_{ik} is the connection weight between i_{th} layer of input, and k_{th} neuron of hidden layer, w_k is the connection weight between k_{th} neuron of hidden layer and single output neuron, b_{hk} is the bias at the k_{th} neuron of hidden layer and b_o is the bias at output layer and P is the predicted output. Transfer function is used to map the weighted sum of the input neuron to the output neuron. In the hidden layer non-linear transfer function Tan sigmoid (Tansig) is used to calculate output. It takes input values in the range of positive and negative infinity and produce output in -1 and 1 range [13]. The Tan sigmoid transfer function is shown in Equation 2. The linear transfer function pure linear (Purelin) is used to calculate output in output layer of neural network architecture. The Purelin transfer function takes input values in the range of positive and negative infinity and produce output in the same range. The Pure linear transfer function is shown in Equation 3.

$$\text{Tansig}(x) = \frac{1 - e^{-2x}}{1 + e^{-2x}} \quad (2)$$

$$\text{Purelin}(x) = y \quad (3)$$

The Mean Squared Error (MSE) is the controlling function for stopping the training process. It is calculated by comparing the measured output (O_m) and predicted output (O_p) value as shown in Equation 4 [14], [15].

$$MSE = 0.5 \sum_{n-1}^{n} (O_m - O_p)^2 \quad (4)$$

The weights are re-adjusted in neural network architecture and training of network is continued till the sum of MSE between target and output layer falls in an acceptable range. The each cycle of training the network is called epochs. In this process the learning rate (ç) is important parameters in training of network. If the learning rate is too small the training will be slow. If the value is large the training of network will not achieve the desired error goal. After various trial and errors optimum value of ç = 0.01 is selected for training [16]. Neural network toolbox (MATLAB version 8.2.0.701) is used for the analysis. A sample of neural network architecture developed in this study is shown in Figure 4.

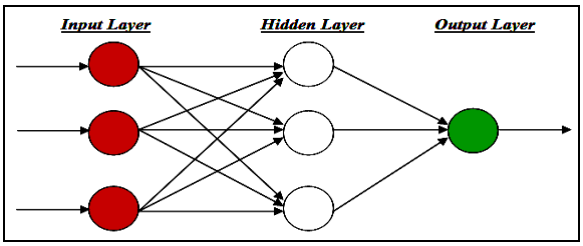

Fig. 4 The ANN architecture

In MATLAB built-in data division function divides total dataset into 70% for training and 30% for validation and testing. To find an optimum architecture for neural network the numbers of neurons in hidden layer are adjusted by trial and error procedure. Hence various models are developed by varying the size of hidden layer for prediction of UCS and E. The R^2 and RMSE are the controlling factors for the selection of optimum models. The results of different models are presented in Table 6. The value of R^2 and RMSE are calculated by Equation 5 and 6.

$$RMSE = \sqrt{\frac{1}{N}\sum_{i=1}^{N} (y - y')^2} \quad (5)$$

$$R^2 = 1 - \frac{\Sigma(y - y')^2}{\Sigma(y - 0)^2} \quad (6)$$

Where measured value is denoted by (y), predicted value (y') and mean ($\bar{y}$) respectively. The RMSE value close to zero and R^2 close to 1 represent that predicted and measured value has minimum error in prediction. The statistical performances of models show that for the prediction of UCS, Regression Model 1, 2 and 3 has R^2 value of 0.53, 0.58 and 0.64 respectively. Neural network model 4, 5 and 6 with same input and output parameters has R^2 value of

Table 6 Results of different models for prediction of UCS and E

Prediction Model	Model	Model Inputs	Network Architecture	Model Output	ANN Analysis	R	R^2	RMSE
Regression	Model 1	$I_{s(50)}$		UCS		0.73	0.53	34.50
	Model 2	RN, $I_{s(50)}$				0.76	0.58	33.39
	Model 3	RN, γ, n, $I_{s(50)}$				0.80	0.64	32.44
ANN	Model 4	$I_{s(50)}$	1-2-1		Training	0.75	0.56	24.19
					Testing	0.68	0.46	
	Model 5	RN, $I_{s(50)}$	2-5-1		Training	0.83	0.69	20.73
					Testing	0.83	0.69	
	Model 6	RN, γ, n, $I_{s(50)}$	4-45-1		Training	0.88	0.77	19.21
					Testing	0.80	0.64	
Regression	Model 1	UCS		E		0.71	0.51	18.34
	Model 2	$I_{s(50)}$, UCS				0.79	0.62	16.08
	Model 3	RN, γ, n, $I_{s(50)}$, UCS				0.81	0.65	15.37
ANN	Model 4	UCS	1-2-1		Training	0.74	0.55	17.86
					Testing	0.71	0.50	
	Model 5	$I_{s(50)}$, UCS	2-5-1		Training	0.86	0.74	15.34
					Testing	0.75	0.56	
	Model 6	RN, γ, n, $I_{s(50)}$, UCS	5-29-1		Training	0.86	0.74	13.59
					Testing	0.88	0.77	

0.56, 0.69 and 0.77 after training of the networks. This indicates significant increase in the R^2 value and non-linear fitting of data by neural network architecture. The results of the same models are further analyzed by calculating RMSE to select the optimum model. After comparing all the models developed with regression and neural network technique lowest value of RMSE is 19.21 of Model 6 predicting UCS. The plot of measured and predicted values of Model 3 (regression) and Model 6 (neural network) is shown in Figure 5. For prediction of E the regression Model 1, 2 and 3 has R^2 value of 0.51, 0.62 and 0.65 respectively. Neural network model 4, 5 and 6 has R^2 value of 0.55, 0.74 and 0.74 after training of the network. This also indicates significant increase in the R^2 value and non-linear fitting of data by neural network architecture. The lowest value of RMSE is 13.59 for Model 6. The plot of measured and predicted values of Model 3 (regression) and Model 6 (neural network) is shown in Figure 6. The RMSE plot is shown in Figure 7.

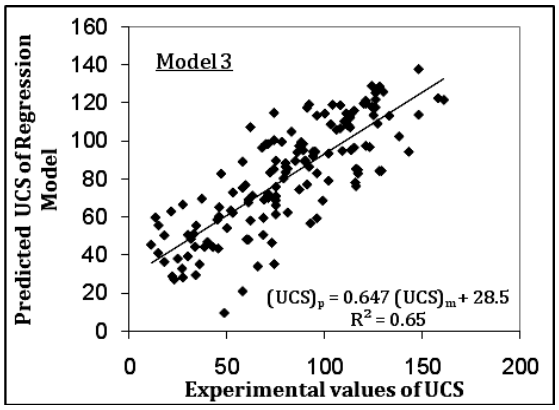

(a)

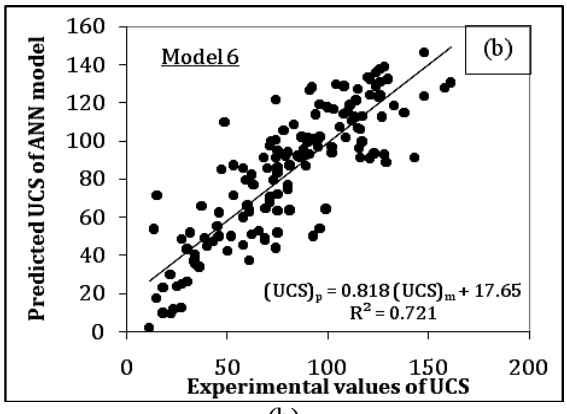

(b)

Fig. 5 Plot of Experimental and Predicted UCS (a) MVRA Model (b) ANN Model

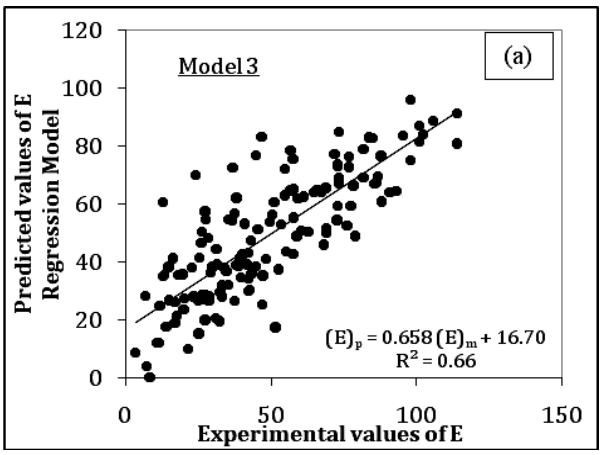

(a)

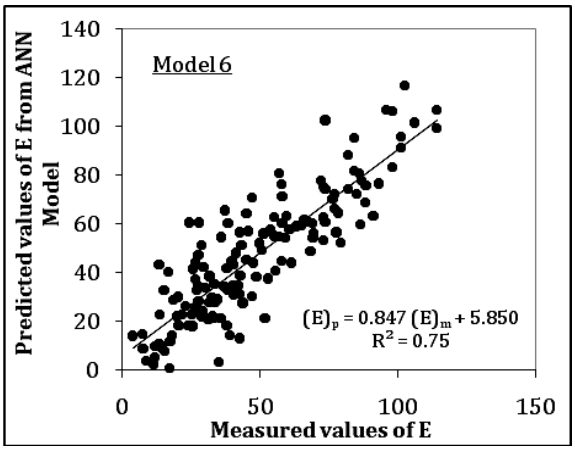

(b)

Fig. 6 Plot of Measured and Predicted E (a) MVRA Model (b) ANN Model

4.2 ANN Model with Two Outputs

ANN has the ability to predict two outputs simultaneously from the input data. The neural network architecture having two neurons in output layer is shown in Figure 8. The values of rock number, unit weight, porosity, point load from the neurons in input layer are transferred to the hidden layer. Two parameters UCS and E are obtained at the output layer. As previously mentioned numbers of neurons in hidden layer are adjusted by trial and error to arrive at optimum network. Neural network toolbox (MATLAB version 8.2.0.701) is used for the analysis. The results of the developed models are presented in Table 7. The assessment of developed models indicate that Model 4 after training has R^2 value of 0.83 and RMSE value of 20.31 and 17.61 respectively for prediction of UCS and E. The values

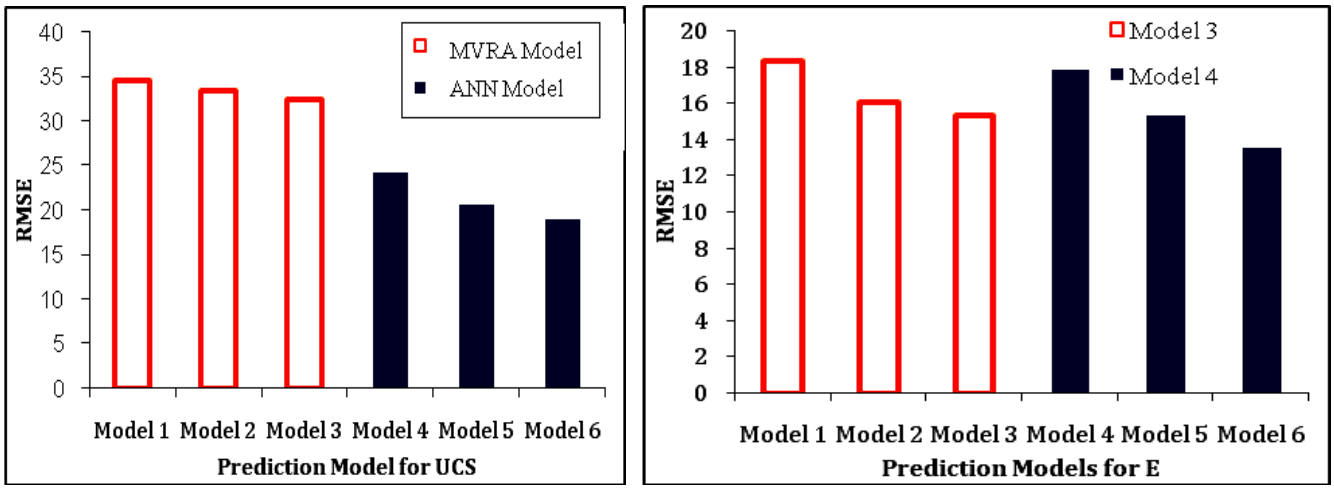

Fig. 7 RMSE plot of MVRA and ANN model (a) UCS (b) E

Table 7 Result of ANN models with neurons in output layer

Network Model	Input Parameter	Output Parameter	Network Architecture	ANN Analysis	*R*	R^2	RMSE	
							UCS	E
Model 1	$Is_{(50)}$	UCS, E	1-12-2	Train	0.84	0.71	23.82	16.86
				Test	0.75	0.56		
Model 2			1-37-2	Train	0.88	0.77	24.23	16.56
				Test	0.62	0.38		
Model 3	RN, γ, n, $Is_{(50)}$	UCS, E	4-7-2	Train	0.82	0.67	22.43	18.45
				Test	0.76	0.58		
Model 4			4-25-2	Train	0.91	0.83	20.31	17.61
				Test	0.65	0.42		

of controlling factors show higher values in comparison to other models. The plot for both predicted and measured values of UCS and E is shown in Figure 9. The RMSE plot is shown in Figure 10.

4.3 Mathematical Formulation of ANN Model

The mathematical equation for prediction of UCS is formulated considering Equation 1 [17]. Weight and biases matrix is obtained from trained neural network Model 6 having network architecture 4-45-1 as discussed in model development section. The Equation 7 is suggested for prediction of UCS. Whereas Tanh and Purelin are transfer function, (IW_{ji}) input weight matrix, (b_{ij}) input bias matrix, (LW) output layer weight matrix and 1.0604 is the output layer bias value. The input layer weight and bias matrix values are shown in Table 8. Similarly the Equation 8 for prediction of E is also suggested utilizing the weight and bias matrix obtained from Model 6 having trained neural network architecture 5-29-1. The input layer weight and biases matrix are shown in Table 9.

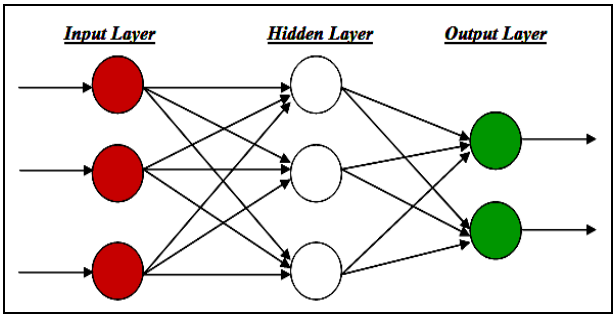

Fig. 8 ANN architecture with two neurons in output layer

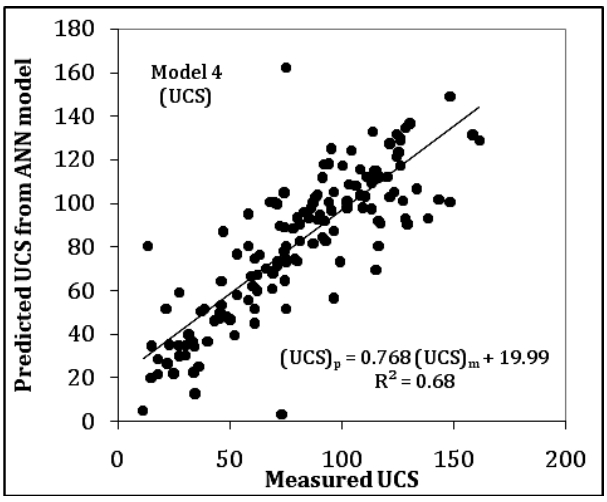

(a)

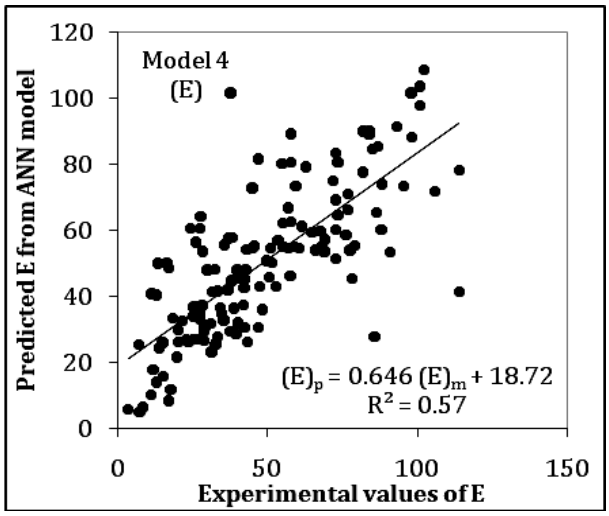

(b)

Fig. 9 Plot of measured and predicted (a) UCS (b) E

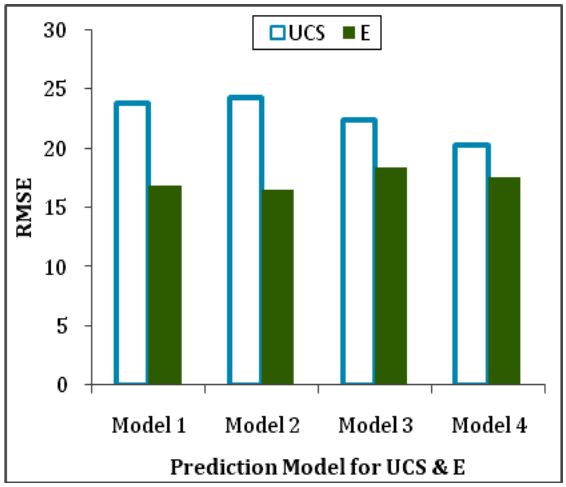

Fig. 10 RMSE plot of ANN model with two neurons in output layer

$$UCS = Purelin[LW\,Tanh[IW_{ji}\,[RN\ \gamma\ n\ Is_{(5)}] + b_{ij}] + 1.0604] \quad (7)$$

$$E = Purelin[LW\,Tanh[IW_{ji}\,[RN\ \gamma\ n\ Is_{(5)}\ UCS] + b_{ij}] - 0.183] \quad (8)$$

Table 8 Weight and Biases values between input hidden layers for UCS model

IW_{ji}				b_{ij}	LW
-0.741	0.990	-2.424	-2.385	3.634	-0.069
1.334	-1.580	2.780	-1.046	-3.635	0.692
2.409	1.272	2.430	-0.092	-3.224	0.560
-0.244	-3.576	0.509	-1.501	1.633	0.492
0.800	1.557	-0.873	-2.933	-2.484	0.225
-1.585	-0.609	-2.203	2.334	3.207	0.724
2.287	-2.428	0.599	1.124	-2.709	0.101
-0.063	-0.205	-2.008	-2.701	-2.683	-0.516
-1.726	1.202	-2.332	-1.705	2.321	-0.086
-0.355	2.532	-2.275	1.244	2.115	-0.243
0.948	2.826	-0.472	-0.738	-2.902	0.719
1.586	2.107	0.223	-1.224	-2.509	0.206
-0.320	2.014	2.342	-1.473	-2.028	0.274
0.791	2.187	-0.383	-2.115	-2.250	0.013
0.825	2.078	-2.612	1.404	-1.055	0.188
1.850	0.554	-0.758	2.927	-1.177	0.364
-2.046	-0.908	1.116	-3.464	1.054	0.020
-0.841	-2.526	2.371	0.454	1.258	0.605
-1.831	0.972	-1.290	3.144	0.482	0.857
1.134	2.781	0.559	-2.047	0.205	-0.320
2.345	-1.203	2.654	1.204	-0.389	0.057
-0.007	2.901	0.918	-1.881	0.195	-0.471
1.327	-1.951	0.696	-2.699	0.163	-0.254
-1.181	-1.454	-0.594	-3.333	-0.518	0.115
0.937	-1.836	-0.435	2.633	0.051	-0.432
-0.694	-2.399	2.143	1.403	-0.396	-0.690
2.595	0.931	-0.898	2.298	0.847	0.496
2.354	-2.231	-0.641	1.331	1.055	0.507
1.681	2.845	-0.466	1.400	1.334	0.225
-1.364	0.108	0.628	-2.368	-0.755	0.104
-2.173	2.748	0.699	-1.088	-0.488	0.160
1.620	-2.816	0.460	-1.415	1.592	0.083
-3.398	1.015	-0.576	-0.055	-1.639	0.637
-2.918	0.740	-0.144	1.971	-1.578	0.611

Table 9 Weight and Biases values between input hidden layers for E model

		IW_{ji}			b_{ij}	LW
0.53	0.70	2.81	-1.09	-0.15	-2.63	-0.29
0.45	1.03	1.77	-1.66	-0.47	-2.60	0.17
-0.08	-0.33	-1.06	-0.25	-2.25	-2.70	-0.50
-1.93	-1.48	-1.32	-0.51	-0.31	1.73	0.26
0.61	2.37	-0.26	-1.13	-1.58	-1.48	0.52
1.31	0.04	-2.02	0.64	-0.47	-1.87	0.09
1.92	-0.75	-0.15	0.55	2.02	-1.53	1.14
-1.60	-1.40	1.70	0.01	-0.40	1.31	0.39
-0.75	0.49	-1.28	1.24	-1.83	1.17	-0.33
-1.92	0.55	-0.72	-1.96	-0.19	0.95	0.03
0.61	1.45	-0.45	1.22	1.98	-0.63	0.40
0.60	-1.17	1.36	-0.70	-1.19	-0.41	-0.42
-0.94	-1.04	1.83	-0.44	1.68	0.89	0.47
1.63	-1.90	-0.63	0.01	-1.06	-0.18	-0.16
1.24	1.57	-0.73	1.54	-0.85	0.19	0.19
0.88	-0.65	1.54	-1.30	-1.71	0.06	0.40
-0.74	-1.09	1.56	1.07	1.50	-0.32	0.46
-1.29	-1.00	1.07	0.94	-0.96	-0.80	-0.13
0.64	0.83	1.43	-0.77	2.03	-0.03	-0.73
2.13	0.00	-0.08	-0.48	-0.92	1.45	0.34
-2.28	-0.27	1.34	-0.53	-0.98	-1.50	-0.26
-1.63	1.38	-0.39	1.66	0.85	-1.35	0.49
1.59	0.72	1.61	0.18	-1.55	1.48	-0.29
0.59	2.31	-0.93	-2.00	0.35	-1.62	0.05
1.91	-1.74	1.16	0.20	0.68	1.88	0.25
1.31	0.37	1.65	0.02	2.13	2.00	0.27
-1.48	1.72	-0.00	-0.55	0.64	-2.97	0.53
-0.99	0.32	-0.05	-2.18	1.03	-2.69	-0.32
-1.59	1.49	-1.22	0.59	-0.04	-2.57	-0.26

5. Conclusion

Four rock index parameters rock type (RN), unit weight (γ), porosity (n), point load ($I_{s(50)}$) are used to predict unconfined compressive strength (UCS) and modulus of elasticity (E). The dataset of igneous and sedimentary rocks prepared after detailed laboratory experimentation is used. The comparison of developed models based on the performance indices of coefficient of determination (R^2), root mean squared error (RMSE) and standard error of estimate (SEE) is as follows.

- The performance indices values of R^2=1, RMSE=1, and SEE=0 were set as target values in order to describe accurate prediction capacity of models.
- The Model 6 of neural network with network architecture 4-45-1 produced R^2, RMSE, SEE of 0.72, 19.2, ± 23% respectively. Regression Model 3 for prediction of UCS produced R^2, RMSE, and SEE of 0.65, 32.44, ± 40%. The ANN Model 6, predicted target values with minimum error and performance indices were close to target range.
- The neural network Model 6 with network architecture 5-29-1 for prediction of E produced R^2, RMSE, SEE 0.75, 13.59, ± 29% respectively. Regression Model 3 for prediction of E produced R^2, RMSE, SEE of 0.66, 15.37, ± 31% respectively.
- The ANN Model 4 with network architecture 4-25-2 produced R^2, RMSE, SEE of 0.68, 20.3, ± 25% for UCS and 0.57, 17.61, ± 35% for E respectively.
- The increase in prediction accuracy of ANN is noted when various laboratory test parameters were introduced. This means generalization capability of ANN increase with large dataset. However for current study the performance of neural network model is significantly higher than the regression model.
- Two separate equations are suggested for the prediction of UCS and E from weights and biases obtained from training of neural networks. It must be noted that equations can be used to predict parameters having same range of dataset as used in the current study.

6. References

[1] *Neural Networks: A Comprehensive Foundation*; Haykin, S., Prentice Hall, N.J, 2nd Edition, (1999).

[2] Liu, S. W., Huang, J. H., Sung, J. C., Lee, C. C. 2002. Detection of cracks using Neural Networks and Computational Mechanics. *Computer Methods in Applied Mechanics and Engineering*. Vol. 191. pp. 2831 – 2845.

[3] Yilmaz, I., Yuksek, A. G. 2008. Technical Note an Example of Artificial Neural Network (ANN) Application for Indirect Estimation of Rock Parameters. *Rock Mechanics and Rock Engineering*. Vol. 41 (5). pp. 781-795.

[4] Yurdakul M, Ceylan H, Akdas H (2011). "A Predictive Model for Uniaxial Compressive Strength of Carbonate Rocks from Schmidt Hardness". 'Civil, Construction and Environmental Engineering Conference Presentation and Proceedings', Paper 7. http://lib.dr.iastate.edu/ccee_conf/7

[5] Yagzi, S., Sezer, E. A., Gokceoglu, C. 2012. Artificial Neural Networks and Non-linear Regression Techniques to Assess the Influence of Slake Durability Cycles on the Prediction of Unconfined Compressive Strength and Modulus of Elasticity for Carbonate Rocks. *International Journal for Numerical and Analytical Methods in Geomechanics*. Vol. 36. pp. 1636-1650.

[6] Majdi, A., Rezaei, M. 2013. Prediction of Unconfined Compressive Strength of Rock surrounding a Roadway using Artificial Neural Network. *Neural Computing & Applications* Vol. 23. pp. 381-389.

[7] Munir, K.; Development of Correlation between Rock Classification System and Modulus of Deformation, Ph.D. Thesis, University of Engineering & Technology, Lahore, Pakistan, (2014).

[8] *Annual Book of ASTM Standards*; D2938-95, D5731-08, ASTM International, West Conshohocken, PA, USA, (2008).

[9] Gul, H.; Prediction Models for Estimation of Unconfined Compressive Strength and Modulus of Elasticity from Index Tests of Rocks, M.Sc. Thesis, University of Engineering & Technology, Lahore, Pakistan, (2015).

[10] Haghnejad, A., Ahangari, K., Noorzad, A. 2014. Investigation on various relations between Uniaxial Compressive Strength, Elasticity and Deformation Modulus of Asmari Formation in Iran. *Arabian Journal for Science and Engineering.* Vol. 39. pp. 2677 – 2682.

[11] Khuntia, S., Mujtaba, H., Patra, C., Farooq, K., Sivakugan, N., Das, B. M. 2015. Prediction of Compaction Parameters of Coarse Grained Soils using Multivariate Adaptive Regression splines (MARS). *International Journal of Geotechnical Engineering.* Vol. 9 (1). pp. 79 -88.

[12] Sulewska M. J. 2010. Prediction Model for Minimum and Maximum Dry Density of Non-Cohesive Soils. *Polish Journal of Environmental Studies.* Vol. 19 (4), pp. 797 - 804.

[13] Guven, A., Gunal, M. 2008. Prediction of Scour Downstream of Grade-Control Structures Using Neural Networks. *Journal of Hydraulic Engineering, ASCE*. Vol. 134 (11). pp. 1656 – 1660.

[14] Mohammadi, H., Rahmannejad, R. 2010. The Estimation of Rock Mass Deformation Modulus Using Regression and Artificial Neural Network Analysis. *Arabian Journal for Science and Engineering.* Vol. 35 (1A). pp. 205-217.

[15] Kabuba, J., Bafbiandi, A. M., Battle, K. 2014. Neural Network Technique for modeling of Cu (II) removal from aqueous solution by Clinoptilolite. *Arabian Journal for Science and Engineering.* Vol. 39. pp. 6793 – 6803.

[16] Khandelwal, M., Singh, T. N. 2011. Predicting elastic properties of schistose rocks from unconfined strength using intelligent approach. *Arabian Journal for Science and Engineering.* Vol. 4. pp. 435 – 442.

[17] Gurocak, Z., Solanki, P., Alemdag, S., Zaman, M. M. 2012. New Considerations for Empirical Estimation of Tensile Strength of Rocks. *Engineering Geology*. Vol. 145 – 146. pp. 1-8.